B. EMG Locations

EMG signals were continuously measured from six muscles of the left lower limb: VL, VM, RF, GM, GL and SOL during the constant workload cycling exercises. The reference electrode was placed over the iliac crest. Fig. 1 illustrated the electrode locations recommended by SENIAM (Surface EMG for Non-Invasive Assessment of Muscles) [12]. A pair of surface bipolar electrodes was attached to the skin with conduct cream at a 20 mm center-to-center electrode distance. The skin at each electrode placement was carefully shaved and cleaned with alcohol to minimize impedance. The lead wires were used to connect the main unit to the electrodes.

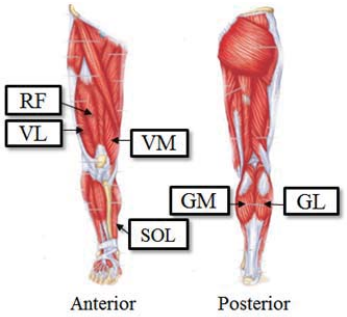

Fig. 1 The EMG electrode locations on the lower limb during cycle upright

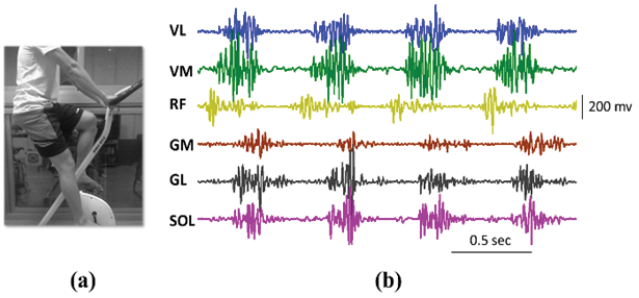

Fig. 2 (a) Subject adjusted the seat height for near full extension of the legs. (b) The EMG signals of six muscles during pedaling exercise

C. Multi-Channel EMG Recording System

The EMG signals were recorded from an amplifier (AURA PSG Wireless/Ambulatory Systems) [13]. The EMG signal was amplified (1000x) and digitized by 10-bit AD converter. The sampling rate of the EMG signal is 200 Hz.

D. Experimental Procedure

Each participant firstly adjusts the saddle height for full leg extension (Fig. 2 (a)) and then performs a constant workload test until failure to maintain the set cadence. The magnetic upright exercise bike (Bike DNA, JT-202) was used in this experiment. It has a monitor to display the current cycling cadence and has eight different levels of workload control.

During the pedaling exercise, all the subjects were informed to pedal at a rhythmic pace and to maintain a constant speed of 90 rpm. Before starting the experiment, each subject was requested to do a warm up (level 1, lightest workload) for 30 seconds to prevent sport injuries. Then the experiment began with a constant workload (level 6, heavy workload). Meanwhile, the EMG signals from six muscles were measured during exercise (Fig. 2 (b)). The experiment was terminated when a subject failed to maintain a rate of 85 rpm for five continuous seconds.

III. Methods

This section presents the methodology of the feature extractions. The flow chart is presented as in Fig. 3. For each EMG channel, a pre-processing step was applied to remove the residual noises and to derive the EMG envelopes of each pedaling. The continuous EMG signals are then decomposed into segments. The features are calculated for all EMG segments.

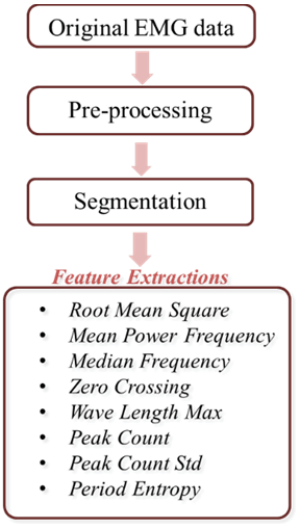

Fig. 3 The flow chart of the proposed feature extraction method

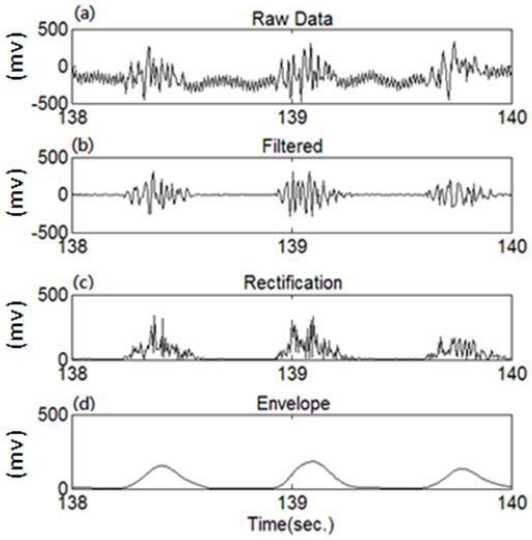

Fig. 4 (a) Original recordings of EMG signal with a 2-second interval. Processing results after (b) filtering (c) rectification and (d) enveloping

A. Pre-Processing Step

In this procedure, a high-pass filter (fourth-order

Butterworth) at 20 Hz and a notch filter at 60 Hz were used to remove the residual noise. Then, the full-wave rectification that turns the negative EMG values to positive is applied. Finally, the EMG envelope is derived by a fourth-order Butterworth low pass filter at 5 Hz. Fig. 4 shows an example of the preprocessing results from the VL EMG signals.

B. EMG Segmentation

In this section, EMG signals were segmented as burst (activation) states and silence (relaxation) states. To identify the activation and relaxation period of each pedal, the average value of the EMG envelops were calculated to determine the activation period. Since the experiment was designed as an isokinetic and rhythmic pedaling exercise (i.e. maintaining at 90 rpm), a simple and straightforward threshold technique could effectively identify the timing of activation and relaxation. In this work, the threshold was set as v =1.7. If the envelope value is greater than 1.7, it means that the muscle condition is in a burst state; otherwise, it is classified as in a silence state. Given the sample index of i^{th} onset and offset as *Onset*(i) and *offset*(i), the center index of the i^{th} AS is defined as:

$$\mathrm{AS}_{center}(i) = \frac{Onset(i)+Offset(i)}{2}. \quad (1)$$

Sequentially, the center index of the i^{th} RS is formulated as:

$$\mathrm{RS}_{center}(i) = \frac{\mathrm{AS}_{center}(i)+\mathrm{AS}_{center}(i+1)}{2}. \quad (2)$$

Besides, the rotation of each pedaling will be consistently sampled between 66 ~ 75 points (sample rate = 200 Hz). In order to avoid capturing the overlapping samples of burst and silence state, a length of 50 points of each segment is recommended in this work. Finally, the samples of the i^{th} AS and the i^{th} RS are respectively defined as:

$$\mathrm{AS}(i) = \{x(AS_{center}(i) - 25), \dots, x(AS_{center}(i) + 24)\}, \quad (3)$$

$$\mathrm{RS}(i) = \{x(RS_{center}(i) - 25), \dots, x(RS_{center}(i) + 24)\}, \quad (4)$$

where $x(\cdot)$ denotes the EMG signals.

C. Feature Extractions

The features introduced in this work are RMS, MPF and MDF, ZC, wave length max (WLM), number and standard deviation (std) of peaks (PC, PCS) and PE. Here, the j^{th} sample of i^{th} EMG segment is defined as $x_i(j)$, and each segment has L sample length (L=50).

1. Root Mean Square

Previous studies show that EMG amplitude oscillation reflects the motor-unit activation, when the level of muscle force is increased [6]. The RMS value has a positive relationship to the increase of pedaling number. The RMS of i^{th} segment is formulated as

$$\mathrm{RMS(i)} = \frac{\sqrt{\sum_{j=1}^{L} x_i(j)^2}}{L} \quad (5)$$

2. MPF and MDF

The muscle fibres of human skeletal muscles can be classified as categories of slow-twitch (Type I) and fast-twitch (Type II). The former has a lower conduction velocity, utilizing power primarily in aerobic (endurance) exercise, like cycling and running, without fatigue. The latter has a higher conduction velocity, utilizing power primarily in anaerobic (heavy) exercise, like bodybuilding and is quickly fatigued [14]. Therefore, the features calculated in the frequency domain might be useful for investigating the progression of the EMG status. The MPF (6) and MDF (7) of i^{th} segment are given as:

$$MPF(i) = \frac{\sum_{j=1}^{M} F(j)P_i(j)}{\sum_{j=1}^{M} F(j)} \quad (6)$$

$$MDF(i) = \underset{F}{arg}\left(\sum_{j=1}^{F} P_i(j) = \frac{1}{2}\sum_{j=1}^{M} P_i(j)\right) \quad (7)$$

where $P_i(j)$ is the EMG segment$_i$ power spectral density at a frequency bin j, $F(j)$ is a frequency value at a frequency bin j and M is the length of frequency bin.

3. Zero Crossing (ZC)

ZC is a feature that records the number of changes the waveform cross zero and is defined as.

$$\mathrm{ZC(i)} = \sum_{j=2}^{L} F\{x_i(j) * x_i(j-1) < 0\} \quad (8)$$

where

$$\mathrm{F}\{A\} = \begin{cases} 1, & if\ A\ is\ true \\ 0, & otherswise \end{cases} \quad (9)$$

ZC is sensitive to polarity changes in signals. A rapid oscillation through baseline within a segment would derive a higher ZC value.

4. Wave Length Max

The WL is defined as the magnitude of two successive samples of a signal, which is calculated as:

$$WL_i(j) = |x(j+1) - x_i(j)| \quad (10)$$

WL is also sensitive to amplitude and frequency variations in the signals. The maximum value of WL of i^{th} segment is used and defined as:

$$WLM(i) = Max(WL_i) \quad (11)$$

5. Number and std Value of Peaks

A peak was defined as a sample point that is either greater than (a top peak) or is smaller than (a bottom peak) its two neighboring samples. The PC is defined as the total number of those top peaks and bottom peaks. The std value of all peaks (PCS) is also used. It was found that the PC decreases when muscle fatigue occurred during a maximum voluntary contraction (MVC) test [15].

6. Period Entropy

In information theory, Shannon entropy is mainly used to estimate an information set which contained the amount of messages [16]. If the samples of space are distributed more uniform, the entropy will be higher. It yields important indications as to the level of disorder in the signal.

Given t is the number of samples between two consecutive bottom peaks, $T = \{ t_1, t_2, \ldots, t_n \}$, where t_k is the t value of the k^{th} and $k+1^{th}$ botom peaks. $p(t)$ is presented as the frequency of t that took place in T.

$$p(t) = \frac{|T(m)=t|}{\sum T} \; \forall m = 1, \ldots, n \tag{12}$$

Finally, PE is formulated as:

$$PE(i) = -\sum_{m=1}^{n} p_i(m) \, log_2 \, p_i(m) \tag{13}$$

D. Data and Statistical Analysis

The exercise period was classified into five stages. That is, the pedal number of each trial was divided to five equal parts (i.e., 0 % - 20 %, 20 % - 40 %, 40 % - 60 %, 60 % - 80 %, 80 % - 100 %). The data of each stage would be analyzed by the segments belonging to their respective part. Data was expressed as mean ± std. One-way ANOVA was applied to present the significant change of the calculated features during exercise.

The p-value is classified as four types:

- $***p<0.001$: high significance
- $0.001<**p<0.01$: moderate significance
- $0.01<*p<0.05$: weak significance
- $p> 0.05$: no significance.

IV. Results

The average pedal number was 414 ± 136 for all subjects. The pedaling number of each trial was dived into five equal stages for performance evaluation. The results of RMS, MPF, MDF, ZC, WLM, PC, PCS and PE were respectively shown and discussed in this section.

A. Results of RMS

A significant change of RMS during constant workload cycling is shown in Fig. 5. It had high significances (p <.001) in the thigh muscles (VL, VM and RF) in the AS segments. The RMS values, as well as the EMG amplitudes become greater with the increasing number of pedal rotations.

B. Results of MPF and MDF

The EMG analysis for muscle condition were commonly analysed through frequency domain (MPF and MDF) during pedaling exercise. The results show that MPF had no significant change in AS and in RS during the pedaling exercise (Fig. 6). Meanwhile, it also reveals that no significant changes were shown in AS and in RS for MDF (Fig. 7).

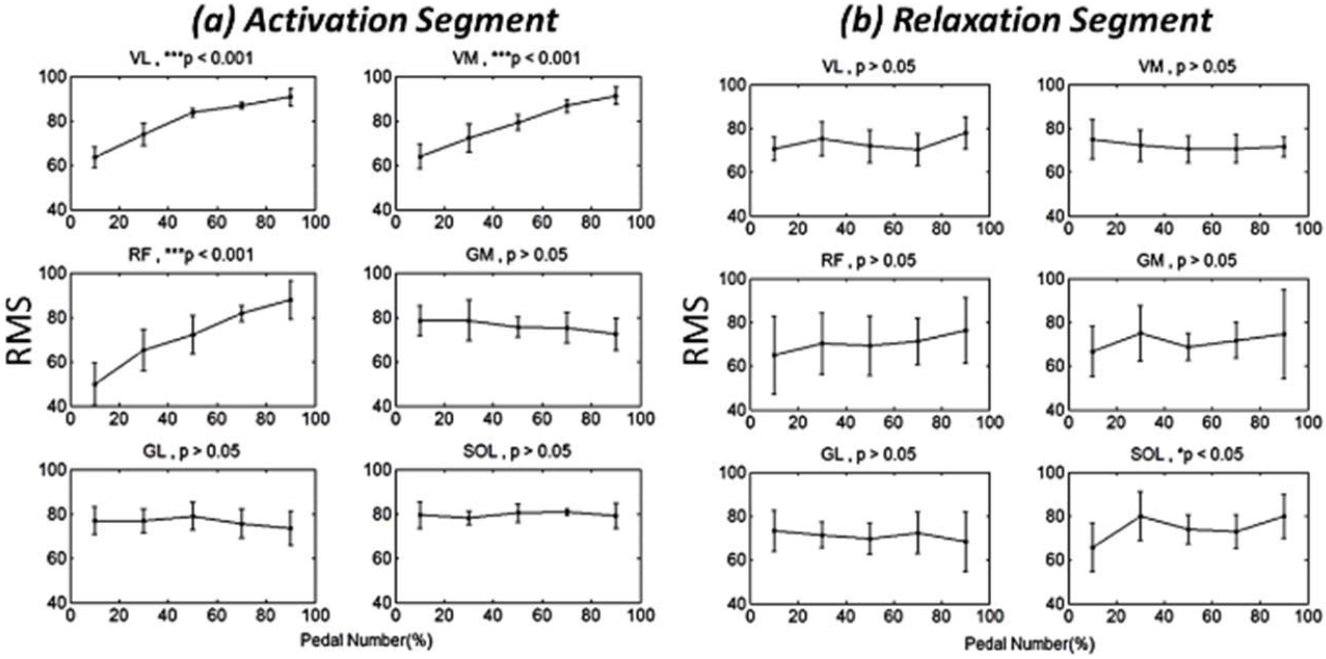

Fig. 5 RMS results of (a) AS and (b) RS. Significant changes were shown when AS were observed

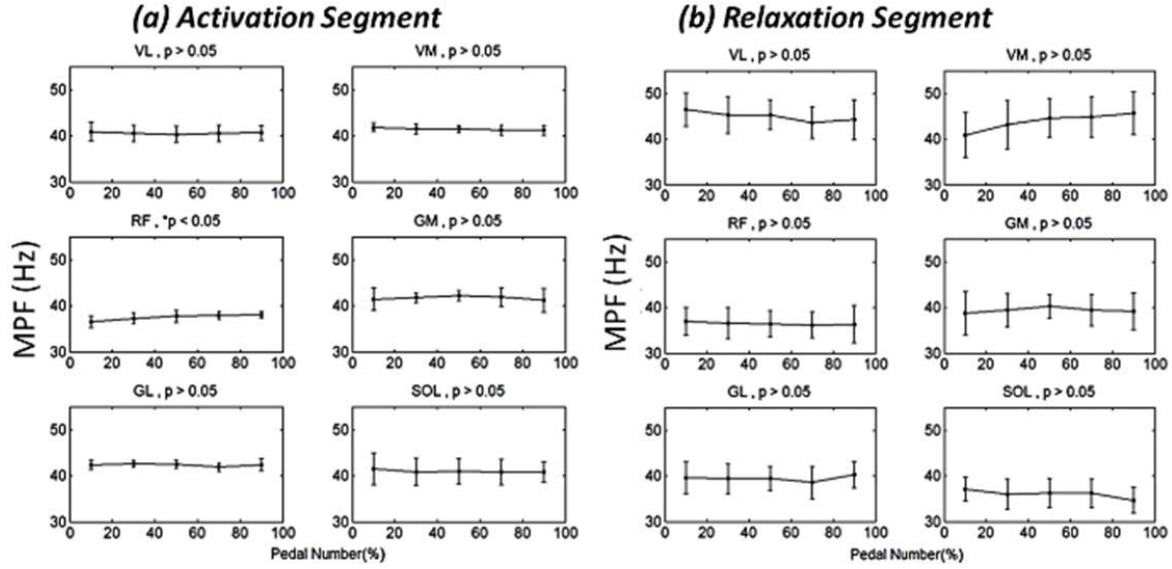

Fig. 6 MPF results of (a) AS and (b) RS. No significant change was found

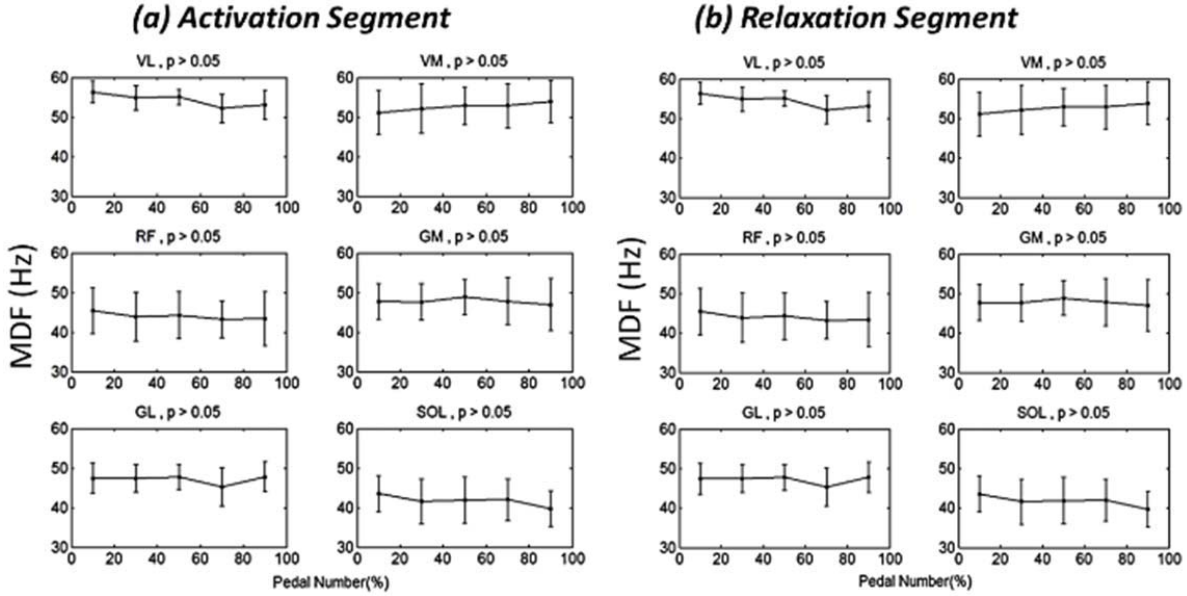

Fig. 7 MDF results of (a) AS and (b) RS. No significant change was found

C. Results of ZC

For ZC, Fig. 8 showed that the significant changes were only presented in RS segments. The ZC value had a high significance in the SOL muscle. With an increase in the number of pedal rotations, the ZC values dropped both in the VL and SOL muscles.

D. Results of WLM

Fig. 9 shows the results of WLM. With the increase in the number of pedal rotations, the WLM were values also elevate. The VL, VM and RF muscles of AS had high significance and the VL of RS had moderate significance.

E. Results of PC and PCS

For PC, moderate significant changes were both shown in VL and SOL of RS (Fig. 10). The PC values dropped along with the increasing number of the pedal rotations.

For PCS, Fig. 11 showed that VL, VM and RF muscles of AS had high significances, and VL of RS also had a high significance. In opposite, the PCS values raised with the increase of the pedal number, that is, the phenomenon of signal fluctuation became prominent during the exercise.

F. Results of PE

In VL muscle of RS, the PE values gradually increased with the rise in the number of pedal rotations (Fig. 12). It means that the period types became more complex and unevenly distributed during exercise.

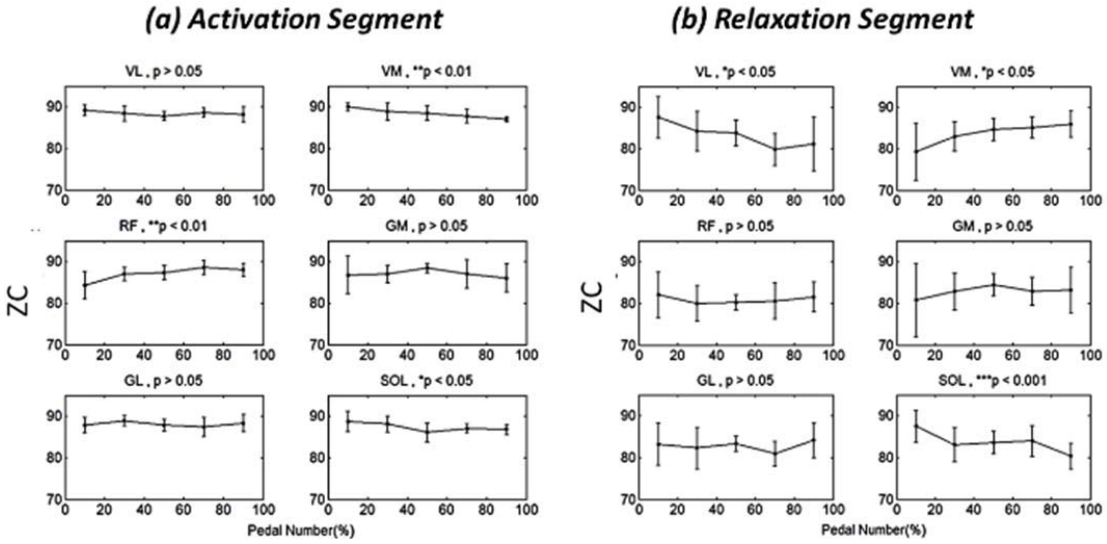

Fig. 8 ZC results of (a) AS and (b) RS. Significant changes were shown when RS were observed

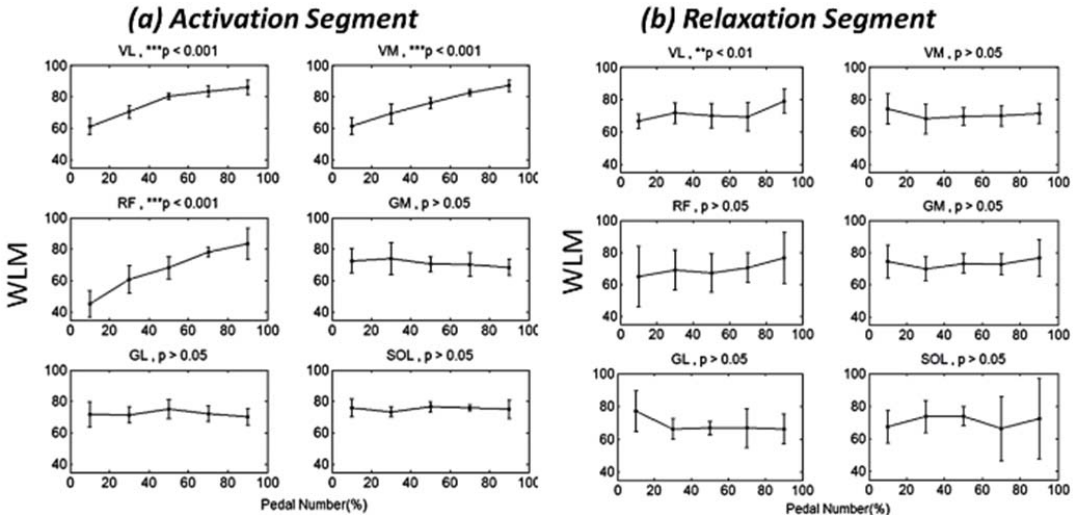

Fig. 9 WLM results of (a) AS and (b) RS. High significant changes were shown in VL, VM and RF of AS. Moderate significant change was shown in VL of RS

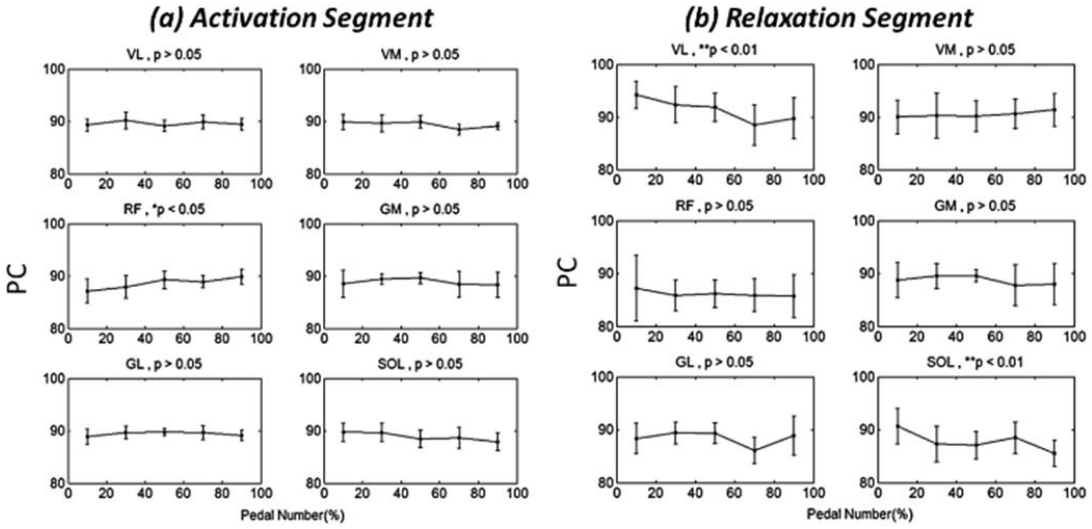

Fig. 10 PC results of (a) AS and (b) RS. Moderate significant changes were shown in VL and SOL of RS

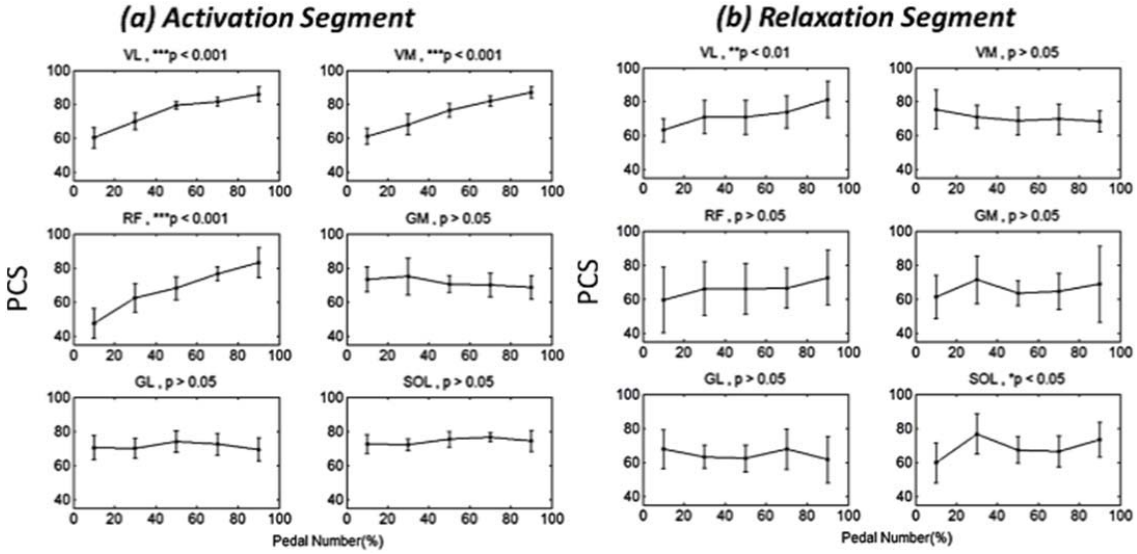

Fig. 11 PCS results of (a) AS and (b) RS

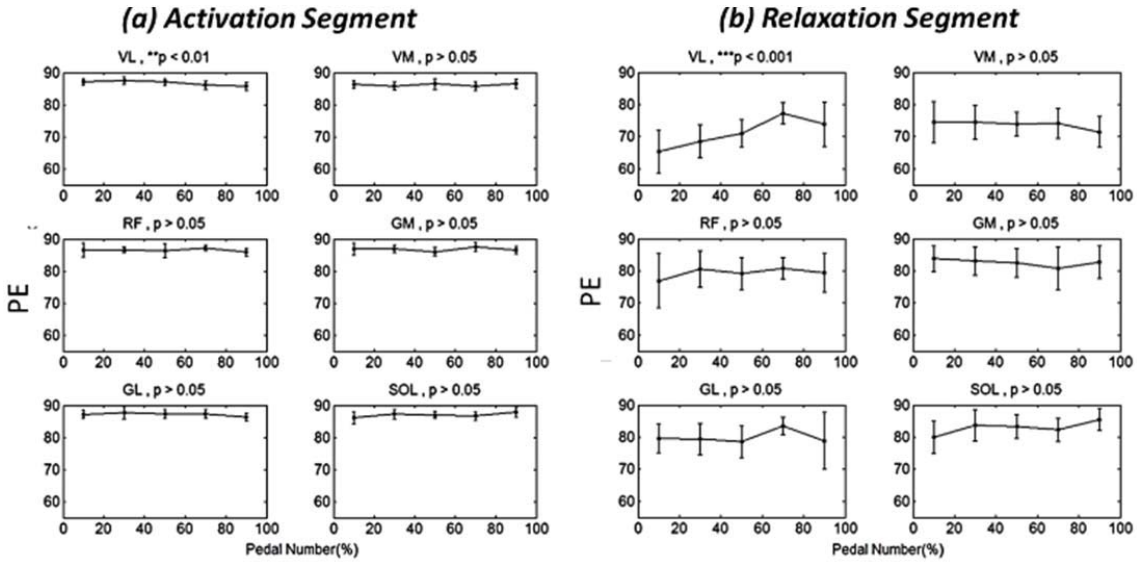

Fig. 12 PE results of (a) AS and (b) RS. A high significant change was shown in VL of RS

G.EMG Changes within Six Muscles

Fig. 13 summarized the relationship among the features, muscles and types of segments. The number of stars means the level of significance calculated by the *p*-value in the results. Three-stars represent the highest significance, two-stars represents moderate significance, while one-star represents weak significance. For the best effects of observation, the stars mostly yield on the VL muscles and therefore VL is recommended for signal analysis during exercise. For RS, it also provided useful information for performance evaluation. Both ZC and PC showed significant changes in SOL when RS was observed.

	Thigh			Calf		
Muscle	VL	VM	RF	GM	GL	SOL
Root Mean Square	***	***	***			
Mean Power Frequency			*			
Median Frequency						
Zero Crossing	*	** *	**			***
Peak Count	**		*			**
Peak Count Std	*** **	***	***			
Wave Length Max	*** **	***	***			
Period Entropy	** ***					
Sum of star signs	24	16	16	0	0	5

* : Activation Segment * : Relaxation Segment

Fig. 13 The comparison of significant changes of 6 muscles during pedaling

V. Conclusions

A feature extraction analysis among six muscles of a constant workload cycling was proposed. The EMG signals in association with five fatigue stages were analyzed. The proposed eight features were investigated to explore the significant changes during cycling. The results found that VL has the most significant changes within the six muscles during the pedaling exercise.

Comparing the AS and RS, the former is usually affected directly by the EMG amplitudes. It was found that the changes of WLM (R^2=0.956) and PVS (R^2=0.970) are pretty similar to RMS in VL muscles. Therefore, it is recommended that RS is also good for performance evaluation. Our results show that the proposed features (i.e., ZC, PC, PCS, WLM and PE) also have promising changes in RS during our cycling experiment.

EMG signals have been widely used to evaluate the level of muscle activation. The proposed features investigated the quantitative information from the EMG signals. The proposed work could be applied to quantify stamina information and predict the instant muscle status of athletes.

Acknowledgment

This work was supported by the Ministry of Science and Technology of Taiwan under Grants MOST 104-2811-E-006-069.

References

[1] J. H. Song, J. W. Jung, Z. and Bien, "Robust EMG pattern recognition to muscular fatigue effect for human-machine interaction." *MICAI 2006: Advances in Artificial Intelligence*. Springer Berlin Heidelberg, 2006. 1190-1199.

[2] B. Fonda, A. Panjan, G. Markovic, N. Sarabon. "Adjusted saddle position counteracts the modified muscle activation patterns during uphill cycling." *Journal of Electromyography and Kinesiology* 21.5 (2011): 854-860.

[3] S. W. Chen, J. W. Liaw, H. L. Chan, Y. J. Chang, C. H. Ku. "A Real-Time Fatigue Monitoring and Analysis System for Lower Extremity Muscles with Cycling Movement." *Sensors* 14.7 (2014): 12410-12424.

[4] S. Minning, C. A. Eliot, T. L. Uhl, T. R. Malone. "EMG analysis of shoulder muscle fatigue during resisted isometric shoulder elevation." *Journal of Electromyography and Kinesiology* 17.2 (2007): 153-159.

[5] A. Meigal, S. Rissanen, M. P. Tarvainen, P. A. Karjalainen, I. A. Iudina-Vassel, O. Airaksinen, M. Kankaanpää. "Novel parameters of surface EMG in patients with Parkinson's disease and healthy young and old controls." *Journal of Electromyography and Kinesiology* 19.3 (2009): e206-e213.

[6] D. Laplaud, F. Hug, and L. Grélot. "Reproducibility of eight lower limb muscles activity level in the course of an incremental pedaling exercise." *Journal of Electromyography and Kinesiology* 16.2 (2006): 158-166.

[7] G. Venugopal, M. Navaneethakrishna, S. Ramakrishnan. "Extraction and analysis of multiple time window features associated with muscle fatigue conditions using sEMG signals." *Expert Systems with Applications* 41.6 (2014): 2652-2659.

[8] T. Migita, and K. Hirakoba. "Effect of switching pedal rate model on slow component of oxygen uptake during heavy-cycle exercise." *BIOLOGY OF SPORT* 24.3 (2007): 191.

[9] M. Navaneethakrishna, S. Ramakrishnan, "Multiscale feature based analysis of surface EMG signals under fatigue and non-fatigue conditions." *International Conference of Medicine and Biology Society (EMBC),* pp. 4627 – 4630, 2014.

[10] M. Vitor-Costa, et al. "EMG spectral analysis of incremental exercise in cyclists and non-cyclists using Fourier and Wavelet transforms." Revista Brasileira de Cineantropometria & Desempenho Humano 14.6 (2012): 660-670.

[11] C. L. Camic, T. J. Housh, G. O. Johnson, C. R. Hendrix, J. M. Zuniga, M. Mielke, R. J. Schmidt. "An EMG frequency-based test for estimating the neuromuscular fatigue threshold during cycle ergometry." *European journal of applied physiology* 108.2 (2010): 337-345.

[12] H. J. Hermens, B. Freriks, C. Disselhorst-Klug, G. Rau. "Development of recommendations for SEMG sensors and sensor placement procedures." *Journal of electromyography and Kinesiology* 10.5 (2000): 361-374.

[13] AURA® PSG LITE, Astro-med Inc., Grass Technologies, West Warwick, RI, USA. http://www.grasstechnologies.com

[14] P. V. Komi, P. Tesch. "EMG frequency spectrum, muscle structure, and fatigue during dynamic contractions in man." *European Journal of Applied Physiology and Occupational Physiology* 42.1 (1979): 41-50.

[15] O. Dayan, S. Irina, E. Amir, G. Pantelis, B. Jeroen, M. Alison "Applying EMG spike and peak counting for a real-time muscle fatigue monitoring system." *IEEE Conference of Biomedical Circuits and Systems (BioCAS)*, pp.41-44, 2012.

[16] T. R. Lee, Y. H. Kim, P.S. Sung. "Spectral and entropy changes for back muscle fatigability following spinal stabilization exercises." *J Rehabil Res Dev* 47.2 (2010): 133-42.